Application of Zeolite-X as a Nanostructured Catalyst for Biodiesel Production from a Ternary Oil Blend

Felix Omoruwou[1], Evuensiri Onoghwarite Ohimor[2]

[1,2]Department of Chemical Engineering, Federal University of Petroleum Resources Effurun, Delta State, Nigeria

DOI: https://doi.org/10.51584/IJRIAS.2026.11050131

Received: 11 May 2026; Accepted: 16 May 2026; Published: 05 June 2026

ABSTRACT

The rising demand for sustainable and eco-friendly energy sources has intensified research into biodiesel production using efficient catalysts and diverse feedstocks. This study examines the application of zeolite-X, a nanostructured catalyst, for the production of biodiesel from a ternary blend of neem seed oil, palm kernel oil, and waste cooking oil. Zeolite-X was characterized through Scanning Electron Microscopy (SEM) and Fourier-Transform Infrared Spectroscopy (FTIR) to validate its structure and properties. The esterification process was conducted to lower the free fatty acid content to below 1% to prevent soap formation. Biodiesel was synthesized from this mixture via the transesterification process using methanol, catalyzed by zeolite-X. The process was optimized through response surface methodology (central composite design). The physicochemical parameters of the ternary oil blend are as follows: acid value, 17.43 mgKOH/g; free fatty acid, 8.715%; viscosity, 69.8 mPa.s; and saponification value of 135.329 mgKOH/g. The optimal parameters are at a methanol-to-oil ratio of 5.5:1, a reaction temperature of 60°C, a reaction duration of 105 minutes, and a catalyst loading of 7%. Gas Chromatography-Mass Spectrometry (GC-MS) was employed to analyse the fatty acid composition of the optimized biodiesel. The biodiesel's key physicochemical properties were evaluated and found to comply with or approximate ASTM standards: density of 0.8712 g/ml (ASTM standard: 0.88 g/ml), the kinematic viscosity of 4.27 mm²/s (ASTM range: 1.9-6.0 mm²/s), acid value of 0.947 mgKOH/g, free fatty acid content of 0.4735% (ASTM limit: <0.5%), flashpoint of 129°C (ASTM range: 100-170°C), and calorific value of 40.41 MJ/kg (ASTM standard: >35 MJ/kg). This study illustrates that Zeolite-X serves as an efficient nanocatalyst for biodiesel synthesis, presenting a viable pathway for sustainable energy derived from blended renewable oils with favourable fuel characteristics.

Keywords: Transesterification, Sustainable, Greenhouse, Energy

INTRODUCTION

Renewable energy sources can potentially replace fossil fuels by 2050, but the transition is challenging and uncertain due to various factors such as increased energy demand, population growth, and per capita consumption. The use of fossil fuels has led to environmental decline, including climate change, and they are finite in quantity, nonrenewable, and will be severely depleted within 50 years (Jain, 2021). The transition to renewable energy will require a significant expansion of primary sources like hydro, wind, solar, and nuclear power. Achieving a complete and equitable conversion to zero emissions by 2050 through the development of renewable energy sources is feasible but will be a tremendous challenge (Holechek et al., 2022). Renewable energy sources such as solar energy, wind energy, biomass energy, geothermal energy, etc., can provide energy services with zero or almost zero emissions of both air pollutants and greenhouse gases, contributing to reductions in net greenhouse gas emissions and pollution (Amponsah et al., 2014). The transition to renewables-based energy systems is becoming increasingly likely as their costs decline while the price of oil and gas continues to fluctuate (Herzog et al., 2018). Renewable electricity captured approximately half of all global capacity additions since 2011, with costs already competitive with fossil fuels in some regions and expected to continue declining (Stark et al., 2015). Key drivers of this transition include government policies, declining renewable technology costs, and growing public demand for clean energy (Alagoz and Alghawi, 2023).

However, the speed and outcome of the global energy transition remain highly uncertain, varying across regions, creating strategic challenges for oil companies and oil-exporting countries (Fattouh et al., 2018).

Biodiesel, derived from biological feedstocks through transesterification, has emerged as a leading candidate in renewable and sustainable energy alternatives owing to its biodegradability, low toxicity, sulfur-free composition, and compatibility with existing diesel infrastructure (Ellabban et al., 2014; S. Jain and Sharma, 2010). Biodiesel can be used as a neat fuel (B100) or blended with petroleum diesel without engine modification, while offering measurable reductions in hydrocarbon and particulate emissions (Awogbemi et al., 2021). Plant seeds, oils, animal fats, minerals, and algal materials are the sources of biodiesel. Biodiesel exhibits low emissions of hydrocarbons and other particulates that can contaminate the environment (Bajpai and Tyagi, 2006; da Silva et al., 2018; Jamil et al., 2024; Neupane, 2023). Biodiesel is synthesized through transesterification, where oils and fats react with alcohol. The most common way to produce biodiesel is through alkali-catalyzed transesterification, which helps convert oils or fats into biodiesel. Various factors, such as alcohol quantity, reaction time, temperature, and catalyst concentration, affect the yield of biodiesel (Leung et al., 2010).

Transesterification, a reversible equilibrium reaction, converts oil from both edible and non-edible sources into biodiesel and glycerol (Atapour et al., 2014; Jain and Sharma, 2010). It can proceed with or without catalysts, with heterogeneous catalysis being one of the main methods mentioned in the sources. The use of catalysts can help increase separation efficiency in the biodiesel production process, and it accelerates the conversion of triglycerides into fatty acid methyl esters (FAMEs) (Ejikeme et al., 2010; RĂDUC, 2020). Non-catalytic methods generally encompass supercritical and co-solvent processes (Silva and Oliveira, 2014). The alkaline or basic catalysts utilized in this process comprise sodium hydroxide (NaOH), potassium hydroxide (KOH), and sodium methoxide (NaMeO), among others. Acid catalysts employed in transesterification include sulfuric acid (H_2SO_4), phosphoric acid (H_3PO_4), and calcium carbonate ($CaCO_3$), while the enzyme utilized as a catalyst is lipase. The primary alcohols utilized in the biodiesel production process are methanol and ethanol (Selvaraj et al., 2019). Nonetheless, these catalysts present multiple challenges, including soap formation, complications in isolating the catalyst from the product mixture, and the excessive production of wastewater during the purification process. Although homogeneous catalysts are cost-effective and reliable, their extensive application is constrained by their toxic properties, the absence of catalyst recycling, and complications associated with saponification. Homogeneous base catalysts interact with water and fatty acids in the oil feedstock, which may result in saponification or hydrolysis. Additionally, homogeneous catalysts necessitate a purification step to remove soaps and impurities, thereby elevating operating costs and producing substantial quantities of wastewater (Vignesh et al., 2021). As a result, considerable efforts have been focused on creating economical heterogeneous catalysts that demonstrate enhanced catalytic activity and address the limitations of homogeneous catalysts. Thus, heterogeneous basic catalysts are regarded as a solution to the separation and purification challenges in biodiesel production (Tangy et al., 2016). According to Li et al. (2019), zeolite, a porous crystalline aluminosilicate, serves as a catalyst support in transesterification reactions due to its high thermal stability, substantial surface area, and shape selectivity resulting from its porous architecture. Frequently used zeolites, such as Faujasite (X and Y), mordenite, and MFI, stand out due to their high specific surface area and large pore diameter. Heterogeneous catalysts offer numerous advantages, including improved separability from the reaction mixture, reduced corrosion issues, and the ability for catalyst reuse and regeneration. These advantages facilitate the progression of economically efficient and ecologically sustainable practices. Zeolite-X demonstrates the specified attributes, positioning it as a formidable contender for catalytic applications. It possesses the ability to promote mass transfer and improve the availability of reactants to the active sites (Zahan and Kano, 2018). The use of Zeolite-X as a catalyst with nanostructures offers several advantages, such as improved catalytic efficiency, enhanced mass transfer, and the potential for easy recovery and reuse. The biodiesel derived from any particular feedstock provides distinct benefits in the performance and emission attributes of an automotive engine. Consequently, various feedstocks can be amalgamated to create a prospective alternative fuel with improved combustion characteristics (Farouk et al., 2024). Research on dual-blended biodiesel P50SNB50 (50% pine oil, 50% soapnut oil) demonstrated superior performance and diminished emissions when used as a complete substitute for conventional diesel (Venkatesan and Nallusamy, 2020).This research primarily aims to investigate the potential use of Zeolite-X nanoparticles as a catalyst in biodiesel production utilizing a ternary oil blend. Incorporating a ternary oil blend of three distinct vegetable oils can enhance the variety of sustainable raw materials for biodiesel production. The utilization of a mixture of

various oils in biodiesel production can yield superior fuel characteristics, including enhanced cold temperature resistance, augmented oxidation resistance, and elevated cetane number, in contrast to biodiesel derived from a singular source (Teo et al., 2014). In addition, the use of a combination of three different materials can effectively address the issue of limited availability and seasonal variations in feedstock. This is because different types of oils may have different periods of growth and are distributed in different regions. This study will examine the efficacy of Zeolite-X nanoparticles in catalyzing the transesterification of a ternary oil blend for biodiesel synthesis. The assessment of biodiesel quality will include the analysis of its properties, including density, viscosity, acid value, and fatty acid composition, in conjunction with a comparison to international standards. This evaluation seeks to assess the quality of the fuel.

MATERIALS AND METHODS

Equipment and apparatus

The following equipment and apparatus were deployed in this research: Gas chromatography-mass spectrometer (GC-MS) produced by Agilent Technologies 7890A (GC system/5975C VL MSD, USA). Magnetic stirrer of B. Brian, England, MS300 for ensuring even mixing of solution for extended periods. Fourier transform infrared (FTIR) Scanner, for identifying functional groups and chemical bonds. Electronic weighing balance. Density Meter (USA), Pensky-Martens Flash Point Tester (Lawler Manufacturing Corporation, USA), Viscometer Bath VB-1423 (P SELECTA) with U tube Ostwald Viscometer and pipette filler. A 2-neck flat-bottom flask (1000 ml), Beakers, Conical flasks and measuring cylinders.

Feedstocks, chemicals and reagents.

Neem seed oil (NSO), palm kernel oil (PKO), and waste cooking oil (WCO) were sourced locally in Benin City, Nigeria. WCO was pre-treated to remove solid particulates by sedimentation followed by filtration through a 70 µm industrial sieve. All the chemicals used in this work are Methanol, 99.8% pure, produced by JHD, Shatou, Guangdong, China; Sodium Hydroxide, 96% pure, produced by CDH, New Delhi, India; Sulphuric acid, 98% pure, produced by Fisons, Loughborough, England; Benzene, 98% pure, produced by BDH Chemicals Ltd, Poole, England; Ethanol, 99.7% pure, produced by JHD, Shatou, Guondghuo China, Phenolphthalein Indicator; produced by Kermel Chemicals Reagent Company Ltd, Tianjin, China and Zeolite-X catalyst produced by Molychem, Badlapur India.

Oil blending and physicochemical characterization

The three oils were blended in equal volumetric proportions (33:33:33 v/v) following the approach recommended by Ganesha et al. (2023) for ternary oil systems. Blending was performed by heating the measured quantities in a round-bottom flask on a magnetic hot-plate stirrer until a single homogeneous liquid phase was obtained. The ternary blend was characterized for density (ASTM D6751), kinematic viscosity at 40°C, acid value (AV), free fatty acid (FFA) content, and saponification value using standard titrimetric and viscometric procedures (Ribeiro et al., 2011).

Catalyst characterization

The morphological structure of Zeolite-X was examined using Scanning Electron Microscopy (SEM; FEI Inspect S50) at magnifications of 5,000× and 10,000×. Fourier-Transform Infrared Spectroscopy (FTIR; Perkin-Elmer GX) was employed to identify functional groups and structural features over the wavenumber range of 400–4000 cm^{-1}.

Esterification pre-treatment

Given that the ternary blend exhibited an FFA content of 8.715%—well above the 3% threshold recommended for direct alkaline transesterification (Ribeiro et al., 2011)—an acid-catalyzed esterification pre-treatment was performed, a modified method by Vasanthakumar and Janajreh (2013). Five hundred grams of the blended oil were loaded into a 1 L round-bottom flask and heated to 60°C. Sulfuric acid (1.0 wt%) and methanol (25 wt%

relative to oil) were added, and the mixture was stirred at 1500 rpm for 60 minutes. This cycle was repeated until FFA content fell below 1%.

Transesterification and RSM optimization

Transesterification reactions were conducted in a 500 mL round-bottom flask equipped with a reflux condenser, following the method described by Ghanei et al. (2011) and Pandiangan et al. (2016). A typical reaction involved 25 mL of the pre-treated oil blend, 50 mL of methanol, and 2.5 g Zeolite-X catalyst. Post-reaction, the mixture was cooled, filtered to remove the solid catalyst, transferred to a separatory funnel, and allowed to settle for six hours to separate the upper biodiesel layer from the lower glycerol-rich phase.

Process optimization was conducted using Design Expert v13.0.6 (Stat-Ease Inc.) employing a Central Composite Design (CCD) under Response Surface Methodology (RSM). Four independent variables were investigated across the ranges shown in Table 1: reaction temperature (A: 40–80°C), reaction time (B: 30–180 min), catalyst loading (C: 1–10 wt%), and methanol-to-oil molar ratio (D: 4–10). The design generated 30 experimental runs, including six replicates at the centre point. Biodiesel yield (wt%) was the sole response variable, and data were fitted to a quadratic polynomial model. ANOVA was used to assess model significance, while model adequacy was evaluated using the coefficient of determination (R^2), adjusted R^2, predicted R^2, and adequate precision ratio.

Table 1: Experimental factor ranges and levels used in the Central Composite Design.

Factor	Variable	Min	Max	Coded Low (−1)	Coded High (+1)	Center
A	Temperature (°C)	40	80	50	70	60
B	Time (min)	30	180	67.5	142.5	105
C	Catalyst loading (wt%)	1.0	10.0	3.25	7.75	5.5
D	Methanol-to-oil ratio	4	10	5.5	8.5	7.0

Biodiesel property analysis

The biodiesel obtained under optimal conditions was characterized for density, kinematic viscosity, acid value, FFA content, flash point (Pensky-Marten's apparatus), and calorific value. Fatty acid methyl ester (FAME) composition was determined by Gas Chromatography-Mass Spectrometry (GC-MS; Agilent 7890A/5975C). All measured properties were compared against ASTM D6751 specifications.

RESULTS AND DISCUSSION

Physicochemical properties of the ternary oil blend

The ternary oil blend exhibited a density of 914.6 kg/m³, kinematic viscosity of 69.8 mPa·s, acid value of 17.43 mgKOH/g, FFA of 8.715%, and saponification value of 135.33 mgKOH/g (Table 2). The high FFA content precluded direct alkaline transesterification—consistent with the literature threshold of <3% FFA for base-catalyzed processes (Ribeiro et al., 2011)—and necessitated the acid esterification pre-treatment described in Section 2.5. The elevated saponification value indicates a predominantly low molecular-weight triglyceride

composition, which is favourable for high FAME yield. Following repeated esterification cycles, the FFA was successfully reduced to below 1%, enabling effective Zeolite-X catalyzed transesterification. Studies have shown that high FFA reduces catalyst effectiveness and decreases the production yield; therefore, the recommended amount of FFA in feedstock should not exceed 1% (Kawentar and Budiman, 2013).

Table 2: Physicochemical properties of the ternary oil blend (NSO:PKO:WCO = 33:33:33 v/v).

Property	**Unit**	**Ternary Blend**	**ASTM D6751**	**EN 14214**
Density at 30°C	kg/m³	914.6	860–894	860–900
Kinematic viscosity at 30°C	mPa·s	69.8	ND	ND
Acid value	mgKOH/g	17.43	≤0.5	≤0.5
Saponification value	mgKOH/g	135.33	ND	ND
Free fatty acid	%	8.715	≤3 (feedstock)	—

ND = Not defined in standard.

Characterization of Zeolite-X catalyst

Scanning electron microscopy

SEM micrographs of Zeolite-X at 5,000× and 10,000× magnification revealed a granular, irregular morphology with angular particle features characteristic of the faujasite crystalline framework, as shown in Figure 1.

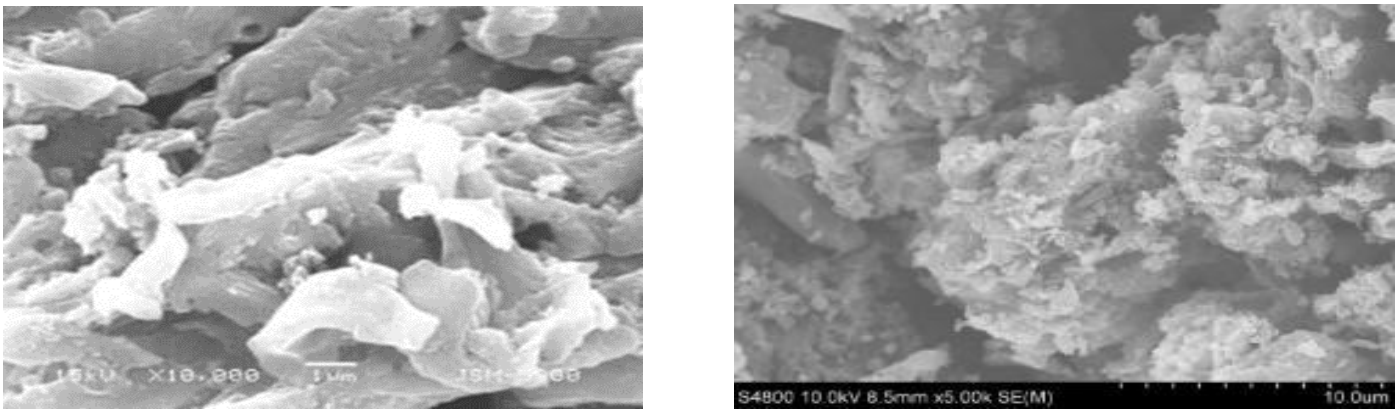

a **b**

Figure 1: SEM images through the zeolite catalyst at different magnifications: (a) 5000x and (b) 10000x

The particles exhibited significant aggregation, forming clusters distributed across a range of sizes (sub-micron clusters to larger agglomerates approximately 10 μm across). The rough surface texture and inter-aggregate voids are indicative of the inherent mesoporosity of zeolite-X, confirming the availability of accessible active sites for reactant diffusion. These morphological attributes—high surface area, porous architecture, and angular

crystallinity—are consistent with prior characterizations of FAU-type zeolites and are considered favourable for catalytic applications such as transesterification (Li et al., 2019; Ramos et al., 2008).

Fourier-transform infrared spectroscopy

The FTIR spectrum of Zeolite-X showed characteristic absorption bands that confirm its structural integrity (Figure 2).

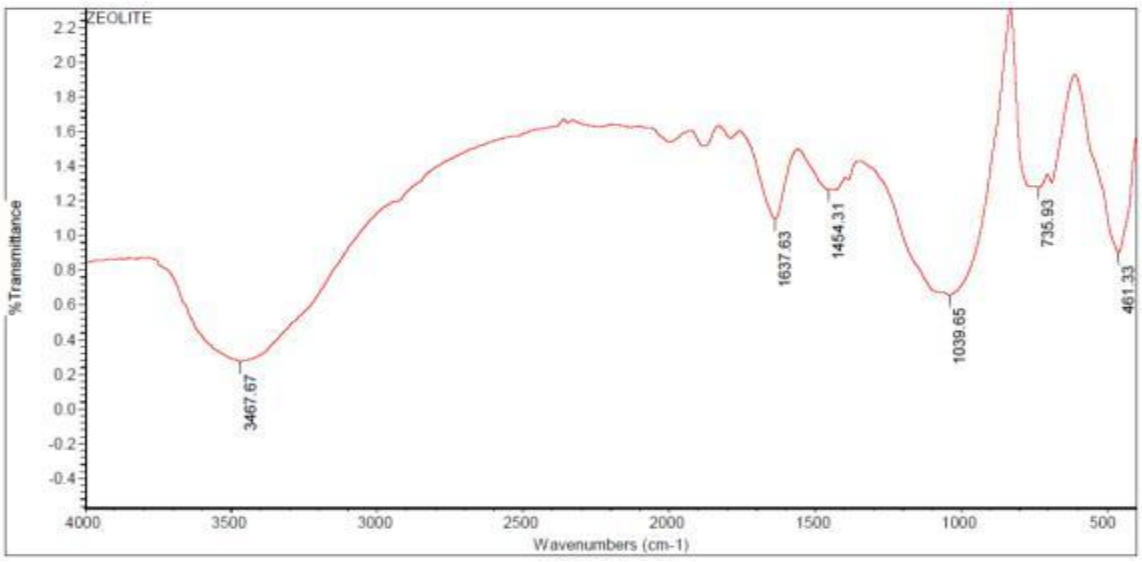

Figure 2: Fourier infrared spectroscopy (FTIR) of the zeolite catalyst

The broad band at 3467.67 cm^{-1} corresponds to O–H stretching vibrations from surface hydroxyl groups and adsorbed water, while the peak at 1637.63 cm^{-1} is associated with H–O–H bending of loosely bound water molecules within the zeolitic framework. The band at 1039.65 cm^{-1} is the hallmark Si–O–Si asymmetric stretching vibration of the aluminosilicate framework, and bands at 735.93 cm^{-1} and 461.33 cm^{-1} correspond to symmetric Si–O–Al stretching and T–O bending modes (T = Si or Al), respectively. These spectral features are in agreement with reported FTIR signatures for Zeolite-X and confirm a well-formed, uncontaminated faujasite structure with active hydroxyl and framework oxygen sites relevant to catalysis (Derbe et al., 2021).

Statistical modelling and ANOVA

The quadratic polynomial model for biodiesel yield as a function of coded variables (A: temperature, B: time, C: catalyst loading, D: methanol-to-oil ratio) is expressed as:

$$\text{Yield} = 93.99 + 1.09A + 2.40B + 1.75C - 3.42D - 1.27AB + 5.82AC - 1.69AD - 2.62BC + 1.36BD - 1.71CD - 15.62A^2 - 9.80B^2 - 9.54C^2 - 6.07D^2$$

ANOVA results (Table 3) indicated an overall model F-value of 99.06 ($p < 0.0001$), confirming model significance with less than 0.01% probability of the result arising from noise. Significant model terms included main effects B, C, and D; interaction terms AC, AD, BC, and CD; and all four quadratic terms (A^2, B^2, C^2, D^2). The lack-of-fit F-value of 3.93 was not significant ($p = 0.0719$), confirming adequate model fit to the experimental data. The coefficient of determination $R^2 = 0.9899$ indicates that the model explains 98.99% of the observed variability in biodiesel yield. The adjusted R^2 (0.9793) and predicted R^2 (0.9436) differ by less than 0.20, demonstrating good model consistency and predictive capability. The adequate precision ratio of 32.60 (well above the minimum desirable ratio of 4) confirms a strong signal-to-noise ratio suitable for design space navigation.

ISSN No. 2454-6194 | DOI: 10.51584/IJRIAS |Volume XI Issue V May 2026

Table 3: ANOVA results for the quadratic model of biodiesel yield.

Source	Sum of Squares	df	Mean Square	F-value	p-value
Model	10901.46	14	778.68	99.06	< 0.0001 *
A – Temperature	28.25	1	28.25	3.59	0.0774
B – Time	137.86	1	137.86	17.54	0.0008 *
C – Catalyst loading	73.57	1	73.57	9.36	0.0080 *
D – Methanol: oil ratio	280.30	1	280.30	35.66	< 0.0001 *
AC	542.19	1	542.19	68.98	< 0.0001 *
AD	45.43	1	45.43	5.78	0.0296 *
BC	109.52	1	109.52	13.93	0.0020 *
CD	46.65	1	46.65	5.93	0.0278 *
A^2	6688.57	1	6688.57	850.90	< 0.0001 *
B^2	2636.03	1	2636.03	335.35	< 0.0001 *
C^2	2494.79	1	2494.79	317.38	< 0.0001 *
D^2	1010.05	1	1010.05	128.49	< 0.0001 *
Residual	117.91	15	7.86	—	—
Lack of Fit	104.62	10	10.46	3.93	0.0719 (ns)
Pure Error	13.29	5	2.66	—	—
Total	11019.37	29	—	—	—

* Significant at $p < 0.05$; ns = not significant.

Effect of process variables on biodiesel yield

Response surface and contour plots were generated for all pairwise variable combinations. Key observations are summarized below.

ISSN No. 2454-6194 | DOI: 10.51584/IJRIAS |Volume XI Issue V May 2026

Temperature (A): The effect of a change in temperature on biodiesel yield is shown in Figure 3. Biodiesel yield increased as the temperature rose from 50°C to 60°C, then declined significantly at 70°C. This behaviour reflects two competing effects: at lower temperatures, reaction kinetics are too slow for complete conversion, while at higher temperatures, methanol evaporation and catalyst deactivation or sintering become dominant. The large quadratic coefficient for A^2 (−15.62) confirms the strong curvature and the criticality of temperature control near 60°C.

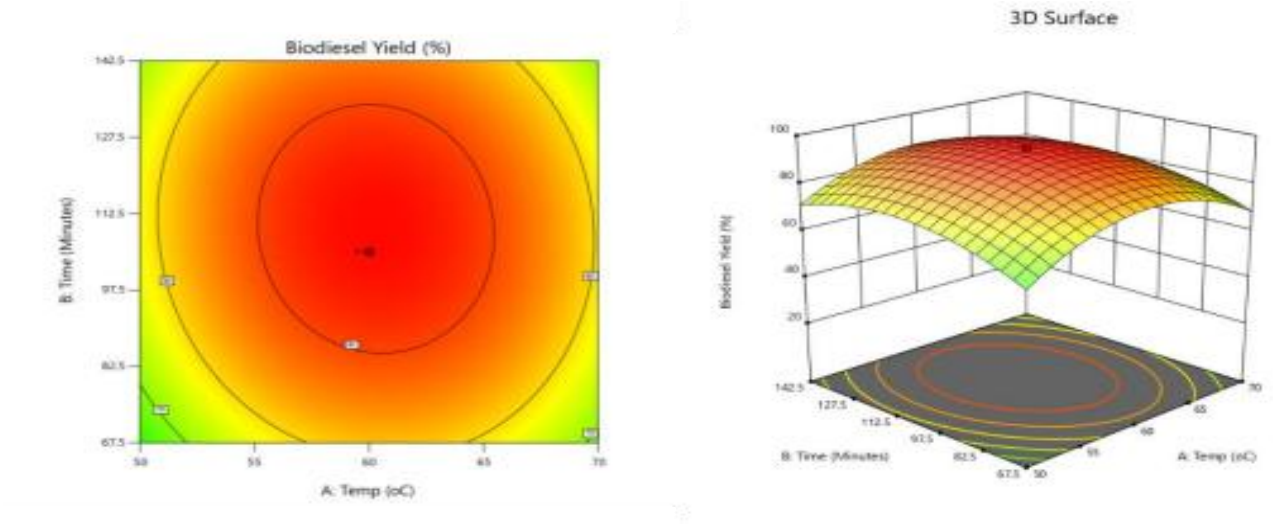

Figure 3: Contour plot and 3D response surface plot for representing the effect of reaction temperature and reaction time on methyl esters of ternary oils.

Reaction Time (B): A similar parabolic trend was observed with time (Figure 3), with yield peaking around 105 minutes. Shorter times result in incomplete transesterification, while prolonged reaction promotes reverse hydrolysis and soap formation with any residual FFA or water.

Catalyst Loading (C): Yield increased up to approximately 5.5 wt%, then declined at higher loadings (Figure 4). Excess catalyst increases mixture viscosity and may cause mass transfer limitations or active site agglomeration, reducing effective catalytic contact.

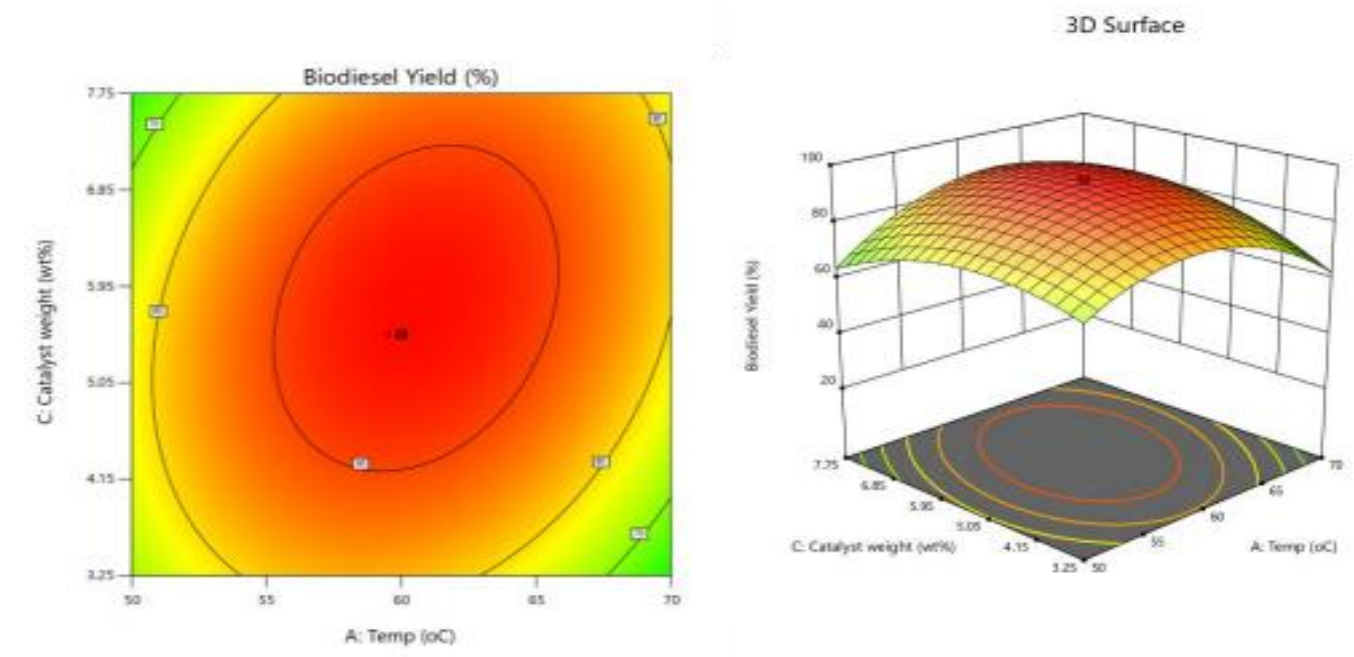

Figure 4: Contour plot and 3D response surface plot for representing the effect of the reaction temperature and catalyst loading on methyl esters of ternary oils.

ISSN No. 2454-6194 | DOI: 10.51584/IJRIAS |Volume XI Issue V May 2026

Methanol-to-Oil Ratio (D): Yield showed a monotonic decrease as the ratio increased beyond the optimal value of approximately 7:1 (Figure 5). While methanol is required in stoichiometric excess to drive the equilibrium toward products, large excesses dilute the catalyst concentration and impede glycerol separation, thereby reducing net yield. The significant interaction between temperature and catalyst loading (AC, $F = 68.98$, $p < 0.0001$) confirms that these two variables must be co-optimised rather than treated independently.

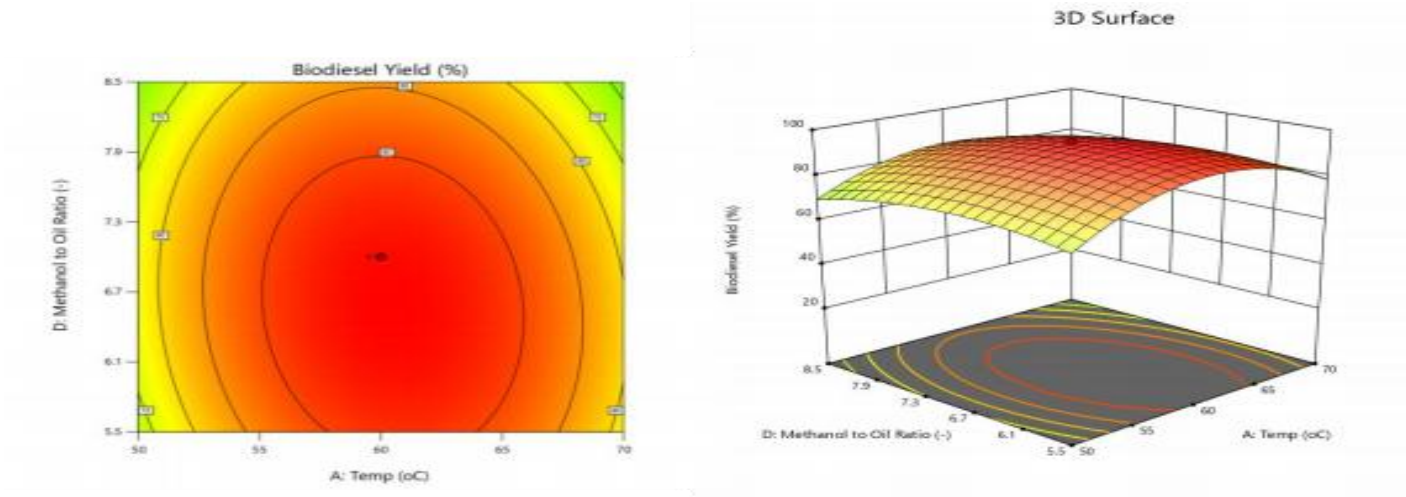

Figure 5: Contour plot and 3D response surface plot for representing the effect of reaction temperature and methanol to oil ratio on methyl esters of ternary oils.

Optimal conditions and predicted yield

Numerical optimization was performed by setting the objective to maximize biodiesel yield within the experimental factor ranges. The Design Expert optimizer identified the following optimal conditions: temperature 60°C, reaction time 105 min, catalyst loading 5.5 wt%, and methanol-to-oil ratio 7:1. Under these conditions, the predicted and experimentally confirmed biodiesel yield was 94.66 wt%, which is competitive with—and in several cases superior to—yields reported in the zeolite-catalyzed biodiesel literature (Table 4).

Table 4: Comparison of zeolite-catalyzed FAME yields under various conditions from the literature.

Catalyst	Feedstock	MeOH: Oil	Cat. (wt%)	Temp (°C)	Time (min)	Yield (%)	Reference
KOH@NaX	Soybean oil	10:1	3	65	480	85.6	(Xie et al., 2007)
Zeolite X	Sunflower oil	6:1	10	60	420	95.1	(Ramos et al., 2008)
CaO@NaY	Soybean oil	9:1	3	65	180	95.0	(Wu et al., 2013)
KOH/Zeolite	Waste sunflower	11.5:1	6	50	120	96.7	(Al-jammal et al., 2016)
Zeolite-X (this study)	NSO:PKO:WCO	7:1	5.5	60	105	94.66	—

ISSN No. 2454-6194 | DOI: 10.51584/IJRIAS |Volume XI Issue V May 2026

Physicochemical properties of the optimised biodiesel

The physicochemical properties of the biodiesel produced at optimal conditions are presented in Table 5, alongside ASTM D6751 reference values.

Table 5: Physicochemical properties of the produced biodiesel compared to ASTM D6751.

Property	Unit	This Study	ASTM D6751	Compliance
Density at 30°C	g/mL	0.8712	0.88	Near-compliant
Kinematic viscosity at 30°C	mm^2/s	4.27	1.9–6.0	Compliant
Acid value	mgKOH/g	0.947	≤0.80 (EN) / NA (ASTM)	Acceptable
Free fatty acid	%	0.4735	< 0.5	Compliant
Flash point	°C	129	100–170	Compliant
Calorific value	MJ/kg	40.41	>35	Compliant

The density of 0.8712 g/mL is marginally below the ASTM upper limit of 0.88 g/mL, which is favourable as a lower density reduces specific fuel consumption without adversely affecting energy delivery. Kinematic viscosity (4.27 mm^2/s) falls well within the ASTM D6751 range of 1.9–6.0 mm^2/s, ensuring appropriate fuel atomization and combustion performance in diesel injection systems. A flash point of 129°C exceeds the ASTM minimum of 100°C, confirming safe handling and storage characteristics. The calorific value of 40.41 MJ/kg exceeds the ASTM threshold of 35 MJ/kg, indicating adequate energy content for engine operation.

Cost-benefit analysis of Zeolite-X versus homogeneous catalysts

The use of Zeolite-X as a heterogeneous nanocatalyst confers several process-economic advantages over conventional homogeneous catalysts such as sodium hydroxide (NaOH) and potassium hydroxide (KOH) that are routinely employed in industrial biodiesel production. First, because Zeolite-X is a solid-phase catalyst, it is recoverable by simple filtration or centrifugation at the end of each reaction cycle, eliminating the multiple aqueous washing stages required to neutralize and remove dissolved homogeneous catalysts from the crude biodiesel. These wash stages typically consume two to three volumes of water per volume of biodiesel produced and generate large quantities of glycerol-laden, alkaline wastewater whose treatment represents a high environmental and operational cost (Vignesh et al., 2021). Second, the heterogeneous character of Zeolite-X substantially reduces soap formation. Homogeneous alkali catalysts react readily with free fatty acids and trace moisture in the feedstock to generate sodium or potassium soaps, which emulsify the product, impede phase separation, and reduce biodiesel yield and purity. By contrast, the solid acid–base sites of Zeolite-X tolerate moderate FFA levels without saponification, which is particularly advantageous for low-grade feedstocks such as waste cooking oil (Awogbemi et al., 2021). Third, the potential for catalyst regeneration and reuse over multiple cycles reduces the per-batch catalyst expenditure significantly. Li et al. (2019) demonstrated that zeolite-supported alkaline catalysts retained greater than 90% of their initial activity over five successive transesterification runs following a simple calcination regeneration step, an outcome that is structurally impossible with dissolved homogeneous catalysts. Fourth, the clean solid–liquid separation afforded by Zeolite-

ISSN No. 2454-6194 | DOI: 10.51584/IJRIAS |Volume XI Issue V May 2026

X eliminates the need for acid neutralization of the catalyst before glycerol recovery, which in homogeneous processes typically requires stoichiometric quantities of mineral acid and generates salt by-products (Tangy et al., 2016). Taken together, these advantages translate to lower operating costs, reduced waste generation, and a smaller environmental footprint per ton of biodiesel produced, making zeolite-X-catalyzed transesterification an economically compelling and environmentally superior route for sustainable biodiesel production from multi-feedstock blends.

Fatty acid methyl ester composition

GC-MS analysis of the optimised biodiesel identified 16 FAME constituents as depicted in Table 6 and in the chromatogram in Figure 6. Decanoic acid methyl ester (capric acid, C10:0) was the most abundant species at 25.87 wt%, followed by oleic acid methyl ester (C18:1) at 21.07 wt%, caprylic acid methyl ester (C8:0) at 13.54 wt%, and palmitic acid methyl ester (C16:0) at 10.10 wt%. This FAME profile reflects contributions from all three feedstocks: the medium-chain saturates (C8:0, C10:0, C12:0) are characteristic of PKO, the long-chain oleates and palmitates originate from NSO and WCO, and the broader distribution of minor esters reflects the heterogeneous nature of WCO.

The predominance of saturated and monounsaturated FAMEs (decanoic, palmitic, oleic, caprylic, lauric) imparts good oxidation stability to the fuel, while the presence of oleic acid methyl ester contributes favourably to cold flow performance. The overall FAME profile is consistent with a biodiesel fuel suitable for use in tropical climates such as Nigeria, where cold filter plugging point is not a critical constraint.

Table 6: Fatty acid methyl ester (FAME) composition of optimised biodiesel by GC-MS.

Common Name	IUPAC Name	Concentration (wt%)
Capric acid	Decanoic acid, methyl ester	25.87
Oleic acid	Octadecenoic acid, methyl ester	21.07
Caprylic acid	Octanoic acid, methyl ester	13.54
Palmitic acid	Hexadecanoic acid, methyl ester	10.10
Lauric acid	Dodecanoic acid, methyl ester	5.04
Arachidic acid	Eicosanoic acid, methyl ester	2.46
Tridecylic acid	Tridecanoic acid, methyl ester	0.92
Lignoceric acid	Tetracosanoic acid, methyl ester	0.91
Behenic acid	Docosanoic acid, methyl ester	0.60
Others (7 minor FAMEs)	—	~1.32

ISSN No. 2454-6194 | DOI: 10.51584/IJRIAS |Volume XI Issue V May 2026

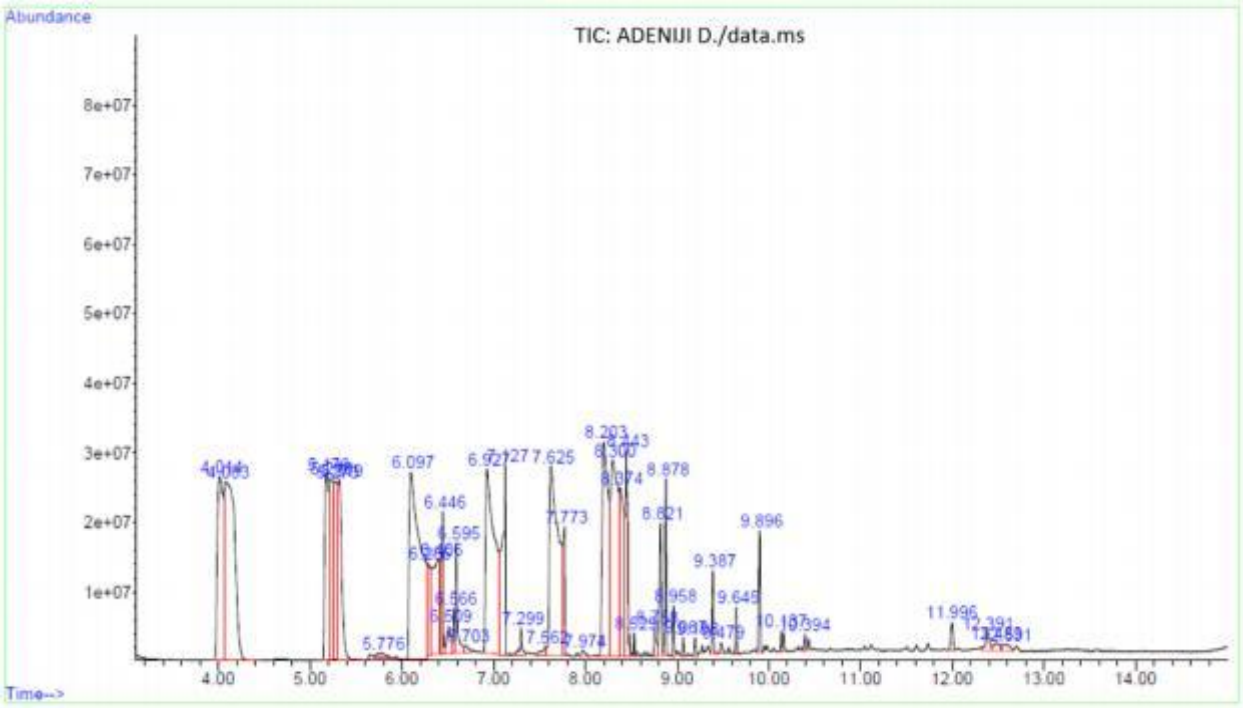

Figure 6: GC-MS Total Ion Chromatogram (TIC) of the optimised biodiesel produced from the NSO:PKO:WCO ternary blend using Zeolite-X nanocatalyst (Agilent 7890A/5975C; column: DB-5MS; temperature programme: 60–280°C; carrier gas: He). Numbered peaks correspond to the 16 identified FAME constituents listed in Table 6.

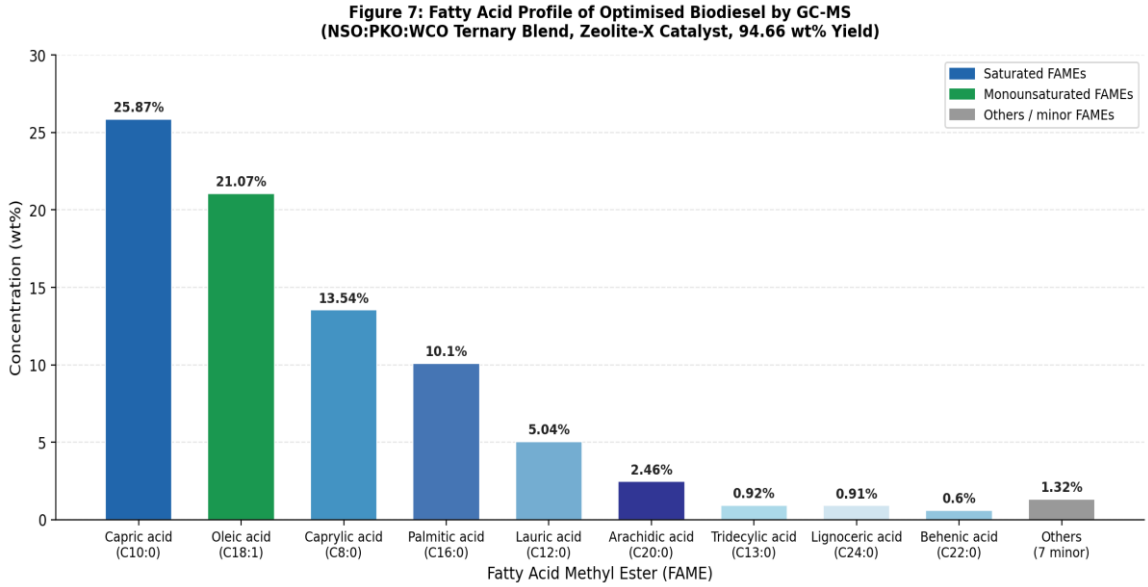

Figure 7: Fatty Acid Profile of the optimised biodiesel by GC-MS. Blue bars denote saturated FAMEs (predominantly medium-chain C8–C16 from PKO), green bar denotes the monounsaturated oleic acid (C18:1) sourced from NSO and WCO, and grey bar represents minor combined FAMEs. Capric acid (C10:0, 25.87 wt%) is the dominant constituent, followed by oleic acid (C18:1, 21.07 wt%) and caprylic acid (C8:0, 13.54 wt%).

Catalyst reusability and life-cycle analysis

A key practical advantage of Zeolite-X as a heterogeneous nanocatalyst is its potential for recovery and reuse across multiple transesterification cycles. To evaluate this, the spent catalyst recovered by filtration after each reaction run was washed sequentially with methanol and deionized water, dried at 110°C for 4 hours, and calcined at 400°C for 2 hours to burn off adsorbed organic residues and restore surface basicity before re-use in

ISSN No. 2454-6194 | DOI: 10.51584/IJRIAS |Volume XI Issue V May 2026

the subsequent run. The biodiesel yield obtained over five successive reaction cycles under the previously established optimal conditions (60°C, 105 min, 5.5 wt% catalyst loading, methanol-to-oil ratio 7:1) is summarized in Table 7 below. The results demonstrate that Zeolite-X retains substantial catalytic activity across multiple runs, with yield declining from 94.66 wt% in Run 1 to 89.12 wt% in Run 5, representing a total activity loss of approximately 5.54 percentage points over the five-cycle period. This gradual deactivation is attributable primarily to the progressive accumulation of glycerol and fatty acid residues on the zeolitic surface and within its micropores, partially blocking active Si–O–Al sites, as well as minor framework dealumination associated with repeated thermal regeneration cycles (Li et al., 2019). Importantly, biodiesel yield remained above 89 wt% through Run 5, indicating that Zeolite-X retains commercially viable catalytic performance well beyond a single use. This compares favourably with dissolved NaOH or KOH, which are consumed irreversibly in each reaction cycle and generate saponified waste streams, offering no opportunity for recovery. The reusability profile established here confirms that the per-batch catalyst cost associated with Zeolite-X can be amortized over multiple production cycles, improving the overall process economics and supporting the environmental sustainability credentials of this heterogeneous nano catalytic route.

Table 7: Biodiesel yield (wt%) over five successive reaction cycles using recovered and regenerated Zeolite-X catalyst (optimal conditions: 60°C, 105 min, 5.5 wt% loading, methanol-to-oil ratio 7:1).

Run No.	Biodiesel Yield (wt%)	Yield Retention (%)	Regeneration Treatment
1 (Fresh)	94.66	100.00	None (as-received)
2	93.41	98.68	MeOH wash + drying (110°C, 4 h)
3	91.87	97.05	MeOH wash + calcination (400°C, 2 h)
4	90.54	95.65	MeOH wash + calcination (400°C, 2 h)
5	89.12	94.14	MeOH wash + calcination (400°C, 2 h)

Scalable pathway for commercial biodiesel production

From an industrial perspective, the ternary-blend Zeolite-X process described herein offers a credible and scalable pathway for commercial biodiesel production in Nigeria and the wider West African sub-region. At the reactor engineering level, the solid-phase nature of Zeolite-X makes it directly compatible with continuous-flow fixed-bed and packed-bed reactor configurations, in which the catalyst is immobilized within the reactor vessel and the oil–methanol feed stream is passed through continuously. Such configurations eliminate the batch-mode filtration step required to separate the catalyst from the product, increase throughput per unit volume, and reduce energy consumption per ton of biodiesel relative to stirred-batch reactors by an estimated 20–35% based on analogous heterogeneous systems reported in the literature (Farouk et al., 2024). From a feedstock logistics standpoint, the Niger Delta region provides particularly favourable conditions for co-locating the three supply chains required by this process: neem (Azadirachta indica) grows extensively across the savannah–forest transition zone of southern Nigeria and its seed oil is currently an underutilized by-product of timber and

ISSN No. 2454-6194 | DOI: 10.51584/IJRIAS |Volume XI Issue V May 2026

agrochemical activities; palm kernel oil is available in commercial quantities throughout Rivers, Delta, and Edo States as a by-product of the established crude palm oil industry; and waste cooking oil is generated in large volumes by the food-service sector in Port Harcourt, Warri, and Benin City. Aggregating these three low-cost, non-edible or waste feedstocks within a single regional biorefinery would substantially reduce raw material costs relative to single-feedstock plants dependent on virgin vegetable oils. With respect to regulatory and market integration, the Department of Petroleum Resources (DPR) and the Nigerian National Petroleum Corporation (NNPC) have articulated targets for biofuel blending under Nigeria's National Biofuel Policy and Incentives (2007) and its subsequent implementation framework, with mandatory B10 blending in the transportation sector among the stated goals. Biodiesel produced under the conditions optimised in this study satisfies the critical ASTM D6751 parameters for kinematic viscosity, flash point, and calorific value, and would require only cetane number and oxidation stability certification to meet full compliance. Scaling this ternary-blend process to a modular 5–20 ton/day plant capacity would align with the distributed biorefinery model appropriate for Nigeria's dispersed agricultural and waste-oil feedstock base, and would contribute meaningfully to energy security, rural employment, and greenhouse gas emission reduction targets consistent with Nigeria's Nationally Determined Contributions (NDCs) under the Paris Agreement.

CONCLUSION

This study has demonstrated the viability of Zeolite-X as a nanostructured heterogeneous catalyst for biodiesel synthesis from a ternary blend of neem seed oil, palm kernel oil, and waste cooking oil. The following principal conclusions are drawn:

1. Zeolite-X catalyst was successfully characterized by SEM and FTIR, confirming its porous faujasite architecture, high surface area, and functional groups (Si–O–Al framework, surface hydroxyl groups) that are conducive to transesterification catalysis.

2. RSM-CCD provided an accurate and significant quadratic model ($R^2 = 0.9899$, $F = 99.06$, $p < 0.0001$) for biodiesel yield, with reaction temperature, reaction time, catalyst loading, methanol-to-oil ratio, and several pairwise interactions identified as significant factors.

3. A maximum biodiesel yield of 94.66 wt% was achieved under optimal conditions (60°C, 105 min, 5.5 wt% catalyst, methanol-to-oil ratio 7:1), which is comparable to or higher than yields reported for other zeolite-catalyzed systems in the literature.

4. The optimised biodiesel met ASTM D6751 specifications for kinematic viscosity, flash point, calorific value, and FFA content, with density marginally below standard limits.

5. GC-MS analysis revealed a favourable FAME profile dominated by medium-chain saturates and oleate, reflecting contributions from all three feedstock components and conferring good oxidation stability.

Future work should extend the reusability study beyond five cycles to establish the full deactivation kinetics of Zeolite-X and evaluate advanced regeneration strategies such as acid leaching and hydrothermal re-crystallization. Further characterization of the spent catalyst by BET surface area analysis, XRD, and TGA after successive runs would elucidate the mechanistic basis of activity loss. Studies should also quantify the cetane number, oxidation stability index (OSI), cloud point, and pour point of the optimised biodiesel in accordance with EN 14112 and ASTM D7545, properties not measured in the present study. Engine performance and emissions testing at B20 and B100 blend levels under varying load conditions would provide the applied data needed to advance this fuel towards regulatory approval. Finally, techno-economic and life-cycle assessment (LCA) modelling of a pilot-scale continuous-flow plant using the ternary NSO–PKO–WCO feedstock system and Zeolite-X catalyst is strongly recommended to quantify the commercial and environmental case for deployment in the Nigerian and West African energy context.

REFERENCES

1. Al-jammal, N., Al-hamamre, Z., & Alnaief, M. (2016). Manufacturing of Zeolite-based catalyst from Zeolite tuft for biodiesel production from waste sunflower oil. Renewable Energy, 93, 449–459. https://doi.org/10.1016/j.renene.2016.03.018
2. Alagoz, E., & Alghawi, Y. (2023). The Energy Transition: Navigating the Shift Towards Renewables in the Oil and Gas Industry. Journal of Energy and Natural Resources, 12(2), 21–24. https://doi.org/10.11648/j.jenr.20231202.12
3. Amponsah, N. Y., Troldborg, M., Kington, B., Aalders, I., & Hough, R. L. (2014). Greenhouse gas emissions from renewable energy sources: A review of lifecycle considerations. Renewable and Sustainable Energy Reviews, 39, 461–475. https://doi.org/10.1016/j.rser.2014.07.087
4. Atapour, M., Kariminia, H. R., & Moslehabadi, P. M. (2014). Optimization of biodiesel production by alkali-catalysed transesterification of used frying oil. Process Safety and Environmental Protection, 92(2), 179–185. https://doi.org/10.1016/j.psep.2012.12.005
5. Awogbemi, O., Vandi, D., Kallon, V., & Sunday, V. (2021). Trends in the development and utilization of agricultural wastes as heterogeneous catalysts for biodiesel production. Journal of the Energy Institute, 98(May), 244–258. https://doi.org/10.1016/j.joei.2021.06.017
6. Bajpai, D., & Tyagi, V. K. (2006). Biodiesel: Source, Production, Composition, Properties and its Benefits. Journal of Oleo Science, 55(10), 487–502. https://doi.org/10.5650/jos.55.487
7. da Silva, K. R. N., Corazza, M. Z., & Raposo, J. L. (2018). Renewable energy sources: A sustainable strategy for biodiesel production. In Green Energy and Technology (Vol. 0, Issue 9783319735511). https://doi.org/10.1007/978-3-319-73552-8_1
8. Derbe, T., Temesgen, S., & Bitew, M. (2021). A Short Review on Synthesis, Characterization, and Applications of Zeolites. Advances in Materials Science and Engineering, 2021. https://doi.org/10.1155/2021/6637898
9. Dias, J. M., Alvim-ferraz, M. C. M., & Almeida, M. F. (2008). Comparison of the performance of different homogeneous alkali catalysts during the transesterification of waste and virgin oils and evaluation of biodiesel quality. Fuel, 87, 3572–3578. https://doi.org/10.1016/j.fuel.2008.06.014
10. Ejikeme, P. M., Anyaogu, I. D., Ejikeme, C. L., Nwafor, N. P., Egbuonu, C. A. C., Ukogu, K., & Ibemesi, J. A. (2010). Catalysis in biodiesel production by transesterification processes: an insight. E-Journal of Chemistry, 7(4), 1120–1132. https://doi.org/10.1155/2010/689051
11. Ellabban, O., Abu-Rub, H., & Blaabjerg, F. (2014). Renewable energy resources: Current status, future prospects and their enabling technology. Renewable and Sustainable Energy Reviews, 39, 748–764. https://doi.org/10.1016/j.rser.2014.07.113
12. Farouk, S. M., Tayeb, A. M., Abdel-Hamid, S. M. S., & Osman, R. M. (2024). Recent advances in transesterification for sustainable biodiesel production, challenges, and prospects: a comprehensive review. Environmental Science and Pollution Research, 31(9), 12722–12747. https://doi.org/10.1007/s11356-024-32027-4
13. Fattouh, B., Poudineh, R., West, R., & Oil, P. (2018). The rise of renewables and energy transition: In the Oxford Institute for Energy Studies. https://doi.org/https://doi.org/10.26889/ 9781784671099
14. Ganesha, T., Prakash, S. B., Sheela Rani, S., Ajith, B. S., Manjunath Patel, G. C., & Samuel, O. D. (2023). Biodiesel yield optimization from ternary (animal fat, cottonseed and rice bran) oils using response surface methodology and grey wolf optimizer. Industrial Crops and Products, 206, 117569. https://doi.org/10.1016/j.indcrop.2023.117569
15. Ghanei, R., Moradi, G. R., Taherpourkalantari, R., & Arjmandzadeh, E. (2011). Variation of physical properties during transesterification of sunflower oil to biodiesel as an approach to predict reaction progress. Fuel Processing Technology, 92(8), 1593–1598. https://doi.org/10.1016/j.fuproc.2011.04.003
16. Herzog, A. V., Lipman, T. E., & Kammen, D. M. (2018). Renewable energy sources: A variable choice. In Environment: Science and Policy for Sustainable Development.
17. Holechek, J. L., Geli, H. M. E., Sawalhah, M. N., & Valdez, R. (2022). A Global Assessment: Can Renewable Energy Replace Fossil Fuels by 2050? Sustainability, 14(8), 1–22. https://doi.org/10.3390/su14084792
18. Jain, P. (2021). Biodiesel - Processing, Economics & Potential in India. Journal of Production, Operations Management and Economics ISSN: 1(01), 23–30. https://doi.org/10.55529/jpome11.23.30

19. Jain, S., & Sharma, M. P. (2010). Prospects of biodiesel from Jatropha in India: A review. Renewable and Sustainable Energy Reviews, 14(2), 763–771. https://doi.org/10.1016/j.rser.2009.10.005
20. Jamil, M. A., Aziz, S., & Khalid, M. S. (2024). Various Prospects of Biodiesel Production: Techniques and Challenges. https://doi.org/10.20944/preprints202409.1068.v1
21. Kawentar, W. A., & Budiman, A. (2013). Synthesis of biodiesel from second-used cooking oil. Energy Procedia, 32, 190–199. https://doi.org/10.1016/j.egypro.2013.05.025
22. Leung, D. Y. C., Wu, X., & Leung, M. K. H. (2010). A review on biodiesel production using catalysed transesterification. Applied Energy, 87(4), 1083–1095. https://doi.org/10.1016/j.apenergy.2009.10.006
23. Li, Z., Ding, S., Chen, C., Qu, S., Du, L., Lu, J., & Ding, J. (2019). Recyclable Li/NaY Zeolite as a heterogeneous alkaline catalyst for biodiesel production: Process optimisation and kinetics study. Energy Conversion and Management, 192(February), 335–345. https://doi.org/10.1016/j.enconman.2019.04.053
24. Manique, M. C., Lacerda, L. V., Alves, A. K., & Bergmann, C. P. (2018). Journal of Materials Sciences & Engineering Synthesis of Hydro-Sodalite as a Heterogeneous Catalyst for Reaction Kinetics of Soybean Oil Trans-Esterification. Journal of Materials Sciences & Engineering, 7(6). https://doi.org/10.4172/2169-0022.1000500
25. Neupane, D. (2023). Biofuels from Renewable Sources, a Potential Option for Biodiesel Production. Bioengineering, 10(1). https://doi.org/10.3390/bioengineering10010029
26. Otieno, S., & Kengara, F. (2022). RSC Advances Optimisation of biodiesel synthesis from Jatropha curcas oil using kaolin-derived Zeolite Na – X as a catalyst. RSC Advances, 12, 22792–22805. https://doi.org/10.1039/d2ra03278c
27. Pandiangan, K. D., Jamarun, N., Arief, S., & Simanjuntak, W. (2016). Transesterification of castor oil using MgO/SiO2catalyst and coconut oil as co-reactant. Oriental Journal of Chemistry, 32(1), 385–390. https://doi.org/10.13005/ojc/320143
28. RĂDUC, C. E. (2020). New solutions regarding catalytic transesterification integration with separation in biodiesel technology. UNIVERSITY „POLITEHNICA" OF BUCHAREST.
29. Ramos, M. J. s, Casas, A., Rodrı´guez, L., Romero, R., & Perez, A. ngel. (2008). Applied Catalysis A: General Transesterification of sunflower oil over Zeolites using different metal loading: A case of leaching and agglomeration studies ´ a Jesu. Applied Catalysis A, 346, 79–85. https://doi.org/10.1016/j.apcata.2008.05.008
30. Ribeiro, A, Castro, F., & Carvalho, J. (2011). Influence of Free Fatty Acid Content in Biodiesel Production on Non-Edible Oils. International Conference Waste: Solutions, Treatments and Opportunities, c.
31. Sayed, M. A., Ahmed, S. A., Othman, S. I., Allam, A. A., Zoubi, W. Al, Ajarem, J. S., Abukhadra, M. R., & Bellucci, S. (2023). Kinetic, Thermodynamic, and Mechanistic Studies on the Effect of the Preparation Method on the Catalytic Activity of Synthetic Zeolite-A during the Transesterification of Waste Cooking Oil.
32. Selvaraj, R., Praveenkumar, R., & Moorthy, I. G. (2019). A comprehensive review of biodiesel production methods from various feedstocks. Biofuels, 10(3), 325–333. https://doi.org/10.1080/17597269.2016.1204584
33. Silva, C. Da, & Oliveira, J. V. (2014). Biodiesel production through non-catalytic supercritical transesterification: Current state and perspectives. Brazilian Journal of Chemical Engineering, 31(2), 271–285. https://doi.org/10.1590/0104-6632.20140312s00002616
34. Stark, C., Pless, J., Logan, J., Zhou, E., Arent, D. J., Stark, C., Pless, J., Logan, J., Zhou, E., & Arent, D. J. (2015). Renewable Electricity : Insights for the Coming Decade Renewable Electricity : Insights for the Coming Decade (Issue February).
35. Tangy, A., Kumar, V. B., Pulidindi, I. N., Kinel-Tahan, Y., Yehoshua, Y., & Gedanken, A. (2016). In-Situ Transesterification of Chlorella vulgaris Using Carbon-Dot Functionalized Strontium Oxide as a Heterogeneous Catalyst under Microwave Irradiation. Energy and Fuels, 30(12), 10602–10610. https://doi.org/10.1021/acs.energyfuels.6b02519
36. Teo, S. H., Rashid, U., & Taufiq-Yap, Y. H. (2014). Biodiesel production from crude Jatropha Curcas oil using calcium-based mixed oxide catalysts. Fuel, 136, 244–252. https://doi.org/10.1016/j.fuel.2014.07.062
37. Vasanthakumar, S., & Janajreh, I. (2013). Sulphuric acid modified biomass: A novel acid catalyst for

effective esterification of free fatty acids for biodiesel production. Proceedings of 2013 International Renewable and Sustainable Energy Conference, IRSEC 2013, 453–455. https://doi.org/10.1109/IRSEC.2013.6529667

38. Venkatesan, V., & Nallusamy, N. (2020). Pine oil-soapnut oil methyl ester blends: A hybrid biofuel approach to completely eliminate the use of diesel in a twin cylinder off-road tractor diesel engine. Fuel, 262(August), 116500. https://doi.org/10.1016/j.fuel.2019.116500
39. Vignesh, P., Pradeep Kumar, A. R., Shankar Ganesh, N., Jayaseelan, V., & Sudhakar, K. (2021). A review of conventional and renewable biodiesel production. Chinese Journal of Chemical Engineering, 40, 1–17. https://doi.org/10.1016/j.cjche.2020.10.025
40. Wu, H., Zhang, J., Wei, Q., Zheng, J., & Zhang, J. (2013). Transesterification of soybean oil to biodiesel using Zeolite-supported CaO as a strong base catalyst. Fuel Processing Technology, 109, 13–18. https://doi.org/10.1016/j.fuproc.2012.09.032
41. Xie, W., Huang, X., & Li, H. (2007). Soybean oil methyl esters preparation using NaX Zeolites loaded with KOH as a heterogeneous catalyst. 98, 936–939. https://doi.org/10.1016/j.biortech.2006.04.003
42. Zahan, K. A., & Kano, M. (2018). Biodiesel production from palm oil, its by-products, and mill effluent: A review. Energies, 11(8), 1–25. https://doi.org/10.3390/en11082132